

A 1D RCE Study of Factors Affecting the Tropical Tropopause Layer and Surface Climate

SALLY DACIE,^a LUKAS KLUFT,^a HAUKE SCHMIDT,^a BJORN STEVENS,^a STEFAN A. BUEHLER,^b PEER J. NOWACK,^c SIMONE DIETMÜLLER,^d N. LUKE ABRAHAM,^{e,f} AND THOMAS BIRNER^g

^a *Max Planck Institute for Meteorology, Hamburg, Germany*

^b *Meteorological Institute, Universität Hamburg, Hamburg, Germany*

^c *Grantham Institute, Department of Physics and the Data Science Institute, Imperial College London, London, United Kingdom*

^d *Deutsches Zentrum für Luft- und Raumfahrt, Institut für Physik der Atmosphäre, Oberpfaffenhofen, Germany*

^e *National Centre for Atmospheric Science, Leeds, United Kingdom*

^f *Department of Chemistry, Centre for Atmospheric Science, University of Cambridge, Cambridge, United Kingdom*

^g *Meteorological Institute, Ludwig-Maximilians-Universität München, Munich, Germany*

(Manuscript received 15 November 2018, in final form 6 June 2019)

ABSTRACT

There are discrepancies between global climate models regarding the evolution of the tropical tropopause layer (TTL) and also whether changes in ozone impact the surface under climate change. We use a 1D clear-sky radiative–convective equilibrium model to determine how a variety of factors can affect the TTL and how they influence surface climate. We develop a new method of convective adjustment, which relaxes the temperature profile toward the moist adiabat and allows for cooling above the level of neutral buoyancy. The TTL temperatures in our model are sensitive to CO₂ concentration, ozone profile, the method of convective adjustment, and the upwelling velocity, which is used to calculate a dynamical cooling rate in the stratosphere. Moreover, the temperature response of the TTL to changes in each of the above factors sometimes depends on the others. The surface temperature response to changes in ozone and upwelling at and above the TTL is also strongly amplified by both stratospheric and tropospheric water vapor changes. With all these influencing factors, it is not surprising that global models disagree with regard to TTL structure and evolution and the influence of ozone changes on surface temperatures. On the other hand, the effect of doubling CO₂ on the surface, including just radiative, water vapor, and lapse-rate feedbacks, is relatively robust to changes in convection, upwelling, or the applied ozone profile.

1. Introduction

There are many uncertainties in tropical tropopause layer (TTL) evolution under global warming, with general circulation modeling studies generally predicting a warming of the cold-point tropopause, but the magnitude of the trend varies greatly between models. The trends found in CMIP5 models for an RCP8.5 scenario are in the range $[-0.5, 3.6]$ K century⁻¹, but the same models produced no identifiable trends over the relatively short time period between 1979 and 2006 (Kim et al. 2013). Observational data from 1970 to 2010 show either a cooling or no significant change (Wang et al.

2012). It is perhaps unsurprising that there is disagreement about TTL evolution, as many models still do not accurately represent all processes affecting the current temperature structure of the TTL. Climatological cold-point temperatures were found to vary in a range of more than 10 K in a comparison of coupled chemistry climate models (Gettelman et al. 2010), and almost the same range of results was found among the CMIP5 models (Kim et al. 2013).

Another disputed topic is whether changes at the TTL are important for surface climate. Some recent studies have focused on how ozone changes expected under global warming might affect changes in surface temperature, but the results of the different studies disagree. Nowack et al. (2015), using a global chemistry climate model, found a reduction in global-mean surface temperature of ~ 1 K due to changes in the ozone profile after 75 years of a $4\times$ CO₂ scenario, while Dietmüller

 Denotes content that is immediately available upon publication as open access.

Corresponding author: Sally Dacie, sally.dacie@mpimet.mpg.de

et al. (2014) found a smaller effect and Marsh et al. (2016) found a negligible effect. Aside from ozone, changes in convection and large-scale circulations could also affect the surface temperature and this could in part occur through changes in the temperature structure and water vapor content of the TTL and the associated changes in longwave absorption and emission.

In this study, we test the importance of CO₂, ozone, large-scale upwelling and convection for the TTL structure and study how the different factors interact with each other. We consider the effect of ozone, upwelling and convection on the equilibrium surface temperature in the tropics, as well as their influence on climate sensitivity.

The factors we have chosen to study are known to be of importance for the TTL, where there is a transition from the convection-dominated troposphere to the stratosphere, which is dominated by radiation and planetary scale dynamics. Radiative heating rates in the TTL are small compared to the rest of the tropical atmosphere, but despite this, they are crucial for determining the temperature structure. Water vapor, CO₂, and ozone have long been considered the most important radiative species (e.g., Manabe and Möller 1961; Gowan 1947; Dobson et al. 1946) and Thuburn and Craig (2002) showed that all three play a role for the structure of the TTL.

Deep convection is also important for TTL temperatures and observational studies (e.g., Johnson and Kriete 1982; Son et al. 2011; Paulik and Birner 2012), provide evidence for this. Isobars increase in altitude within clouds, due to convective heating, and Holloway and Neelin (2007) proposed that the pressure anomaly also extends above the convective heating. They further argued that the horizontal pressure gradients above the cloud top lead to divergence and large-scale upward motion, producing adiabatic cooling. Other processes could also contribute to the cooling required to reduce the pressure gradients. The modeling study of Kuang and Bretherton (2004) provides evidence for cooling via overshooting convection (Sherwood and Dessler 2000), and cloud radiative effects may also contribute to cooling. In this case, the large-scale upward motion would weaken to maintain the same total cooling (Holloway and Neelin 2007).

Large-scale adiabatic cooling is also produced by the tropical upwelling associated with the Brewer–Dobson circulation. Many modeling studies have found a strengthening of the Brewer–Dobson circulation with global warming (e.g., Butchart et al. 2006; Garcia and Randel 2008), but it is not clear how large any changes would be and Oberländer-Hayn et al. (2016) found no change in tropical upwelling strength when considered

with respect to the changing tropopause pressure. Any changes in deep convection and large-scale circulation would likely alter the temperature structure of the TTL directly, as well as indirectly by affecting the atmospheric composition, including water vapor and ozone concentrations.

In this study, we choose to use a 1D clear-sky radiative–convective equilibrium (RCE) model. This kind of model has the advantage that it can be run to numerical equilibrium at a high vertical resolution at low computational cost. Therefore, it is very well suited to parameter studies, so the role of different factors and their interactions can be explored.

There have been a number of previous 1D RCE modeling studies, but only a few focus on the tropopause region. Thuburn and Craig (2002) carried out an extensive parameter study, investigating the effects of CO₂ concentration, relative humidity, ozone profile, tropospheric lapse rate and large-scale dynamical cooling. Fu et al. (2018) repeated some of these experiments and additionally studied cloud radiative effects on the TTL. Birner and Charlesworth (2017) focused on the relative roles of dynamical cooling due to Brewer–Dobson upwelling and modifications of radiative heating due to shifted ozone profiles. All three of these studies used a model with a fixed surface temperature, so could not investigate mechanisms linking the tropopause with surface temperature. On the other hand, McElroy et al. (1992) used a model with an interactive surface to study the surface temperature dependence on the ozone profile. However, this study included only three ozone profiles and did not test any other factors. None of these 1D TTL studies investigated the role of convection, and here we do this by using two different methods of convective adjustment, each following a few simple assumptions.

Despite the advantages discussed above, 1D RCE models also have limitations, namely that they have no explicit dynamics or transport, and in our case as well as in three of the four studies mentioned above, no clouds.

The model setup is described in section 2 and our idealized experiments, designed to study the influence of different factors on the equilibrium state, are described in sections 3–6. In section 3, we study the effect of changing the CO₂ concentration on the TTL structure. Then in section 4, we study the effect of vertical shifts in the ozone profile on the temperature profile of the TTL and on surface temperatures. The effect of an adiabatic cooling associated with an upwelling is described in section 5 and in section 6 we study the combined effect of these three possible changes. In section 7, we investigate the temporal evolution of the cold point to an instantaneous CO₂ perturbation. In section 8, we apply

our model to the question of whether ozone profile changes predicted by coupled chemistry climate models affect climate sensitivity and here we show a large influence of the model setup. We discuss our results, the importance of model assumptions and the assumptions made in analysis techniques in [section 9](#).

2. Model setup

We use the 1D RCE model of [Kluft et al. \(2019\)](#) (v0.6.6, available at github.com/atmtools/konrad), which runs on pressure coordinates with 200 levels and a spacing that increases linearly in logarithmic pressure space to a model top at 0.01 hPa. The surface in the model is a simple slab surface characterized by its heat capacity, but as the heat capacity only affects the temporal evolution of the model, it is not important for this study, where most of the results are taken from equilibrium states. The results regarding the temporal evolution ([section 7](#)) are also found to be qualitatively similar for a wide range of surface heat capacities.

In this study, we use a setup with a constant value of relative humidity throughout the troposphere. We choose a relative humidity of 0.40, as this is approximately equal to tropical-mean upper-tropospheric humidity in ERA5 data. Above the cold-point tropopause in the stratosphere, we use a fixed water vapor volume mixing ratio set by the temperature and relative humidity at the cold point. Although this profile is unrealistic in several aspects, we choose it for its simplicity and the way it responds to changes in atmospheric temperature. If the troposphere warms and deepens, and the cold point moves upward to a lower pressure retaining the same temperature, the region with a relative humidity of 0.40 also deepens, in agreement with the conceptual model of [Romps \(2014\)](#). On the other hand, if the cold point cools, the stratospheric humidity decreases, as expected. Unless otherwise specified, all of the runs performed for this study use this humidity setup.

The other trace-gas concentrations are those specified in [Wing et al. \(2018\)](#), including a CO₂ concentration of 348 ppmv and an ozone concentration profile given by an analytic approximation to an annual-mean equatorial climatology. For the solar insolation, we use a tropical-mean zenith angle of 42.05° ([Wing et al. 2018](#)) and a reduced solar constant of 480 W m⁻², to avoid unrealistically high temperatures in a model with no meridional heat transport. The RRTMG radiation scheme ([Mlawer et al. 1997](#)) is used to calculate the radiative heating rates, which we apply at each time step to give us the temperature profile T_{rad} , and this is followed by a convective adjustment in the troposphere. Many 1D RCE models use a convective adjustment to restore the tropospheric

lapse rate to the moist adiabat [first used in a 1D RCE study by [Hummel and Kuhn \(1981\)](#)] at each time step. Our implementation of this is described in the appendix of [Kluft et al. \(2019\)](#) and in this study we refer to this method as the hard convective adjustment. Here we make comparisons to runs using a different convective adjustment ([section 2a](#)), where we have relaxed this constraint. Regardless of the convective adjustment type, the only feedbacks in our model are from the radiation scheme (e.g., the Planck feedback), water vapor amount, and the lapse rate, as these are the only temperature dependent factors in the model.

We define the TTL between our convective top ([section 2b](#)) and the cold point, and we quantify TTL changes based on these two points, following [Thuburn and Craig \(2002\)](#).

a. Relaxed convection

In this section, we introduce a method of performing the convective adjustment, and by comparing this to the established hard adjustment method (detailed in the appendix of [Kluft et al. \(2019\)](#), we can test how different but reasonable assumptions related to convection affect our results.

Convection in the real atmosphere occurs on a range of time scales, with shallow convection acting frequently and quickly over small vertical scales, and with deeper convection requiring more time to develop. Then, the mean convective heating profile can be seen as a combination of the profiles from numerous convective plumes, which extend to a variety of heights. To mimic this, we define a convective temperature increment ΔT as a function of pressure p , such that convection weakens with height:

$$\begin{aligned} \Delta T(p) &= T_{\text{con}}(p) - T_{\text{rad}}(p) \\ &= \Delta T_{\text{hard}}(p)R(p), \end{aligned} \quad (1)$$

with the subscripts rad and con for the radiatively and convectively adjusted profiles respectively, $\Delta T_{\text{hard}}(p)$ the temperature change for a hard adjustment, and $R(p)$ a relaxation factor [$0 \leq R(p) \leq 1$]. This temperature change is given by

$$\Delta T_{\text{hard}}(p) = T_{\text{con},s} - \int_{p_s}^p \gamma_p dp - T_{\text{rad}}(p), \quad (2)$$

where the subscript s stands for surface and γ_p is a specified lapse rate (temperature change with respect to pressure), which we choose to be the moist adiabat. The relaxation factor is given by

$$R(p) = 1 - e^{-t/\tau(p)}, \quad (3)$$

where t is the time step, and $\tau(p)$ is a convective time scale. Thus, in the relaxed adjustment case for $\tau(p) \neq 0$,

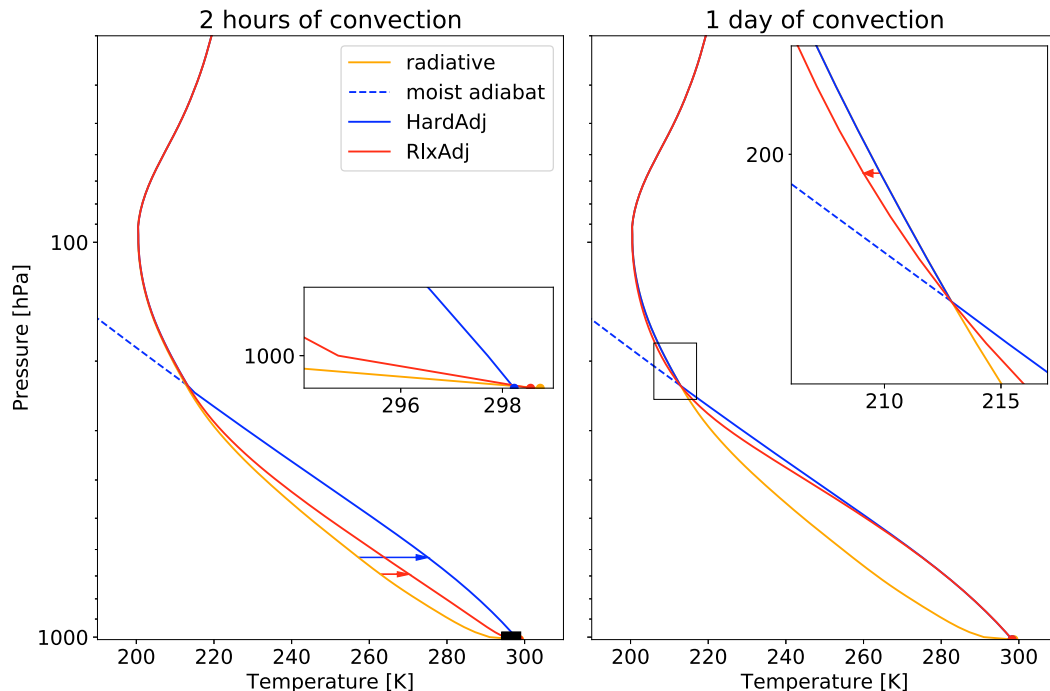


FIG. 1. A comparison of the hard adjustment (HardAdj; blue) and the relaxed convective adjustment (RlxAdj; red), with the radiative profile shown in orange. The radiative profile results from turning off convection for 20 model days: it is not radiative equilibrium, nor is it the radiative profile after a single model iteration, which would barely differ from radiative–convective equilibrium. The convectively adjusted profiles (left) after 2 model hours of convection and (right) after 1 day of convection. The zoom box of the left panel shows the region close to the surface (black rectangle on the main plot), with surface temperatures indicated by dots. The zoom box of the right panel shows the region around the top of convection, above which HardAdj is equal to the radiative profile, but RlxAdj is between the radiative profile and the moist adiabat. The horizontal blue and red arrows show $\Delta T_{\text{hard}}(p)$ and $\Delta T(p) = \Delta T_{\text{hard}}(p)R(p)$, respectively.

our temperature change is smaller than for the hard adjustment in the troposphere. Another difference between the hard and relaxed adjustments, is that the hard adjustment is only applied up to a certain model level, namely the level of neutral buoyancy (where a rising air parcel has the same density as its environment), which is determined by the lapse rate and energy conservation. In contrast, the relaxed adjustment is applied throughout the whole column. $\Delta T(p)$ and $\Delta T_{\text{hard}}(p)$ are depicted as red and blue horizontal arrows in Fig. 1.

The relaxed adjustment gives us a convective temperature profile of

$$T_{\text{con}}(p) = T_{\text{rad}}(p)e^{-t/\tau(p)} + [1 - e^{-t/\tau(p)}] \left(T_{\text{con},s} - \int_{p_s}^p \gamma_p dp \right), \quad (4)$$

which is valid for the whole atmosphere, but it is closely linked to the radiative temperature profile for large $\tau(p)$. As $\tau(p)$ becomes much larger than the radiative time scale, the convection can no longer change the temperature profile and $T_{\text{con}}(p) = T_{\text{rad}}(p)$.

The profile we choose for τ is as follows:

$$\tau(p) = \tau_0 e^{p_0/p}, \quad (5)$$

with p_0 the pressure of the lowest atmospheric level (set as 1000 hPa). τ_0 is set to 1 h, on the order of the convective adjustment time used in several convection schemes and found to reproduce observations well (e.g., Betts and Miller 1986). As τ increases with height, the influence of convection weakens, thus we may expect other factors (e.g., changes in radiative heating due to a shifted ozone profile) to have a larger impact.

Our choice of τ is tuned for our standard model setup and there is no reason to believe that it is suitable for other climate states. Nevertheless, as there is currently no sound theoretical basis about how the time scale of convection might change, we assume that τ stays fixed with pressure and does not change as we perturb other factors. Regardless of the assumptions about τ , comparisons between the hard and relaxed adjustments allow us to study whether reducing the importance of convection in the upper troposphere in the relaxed

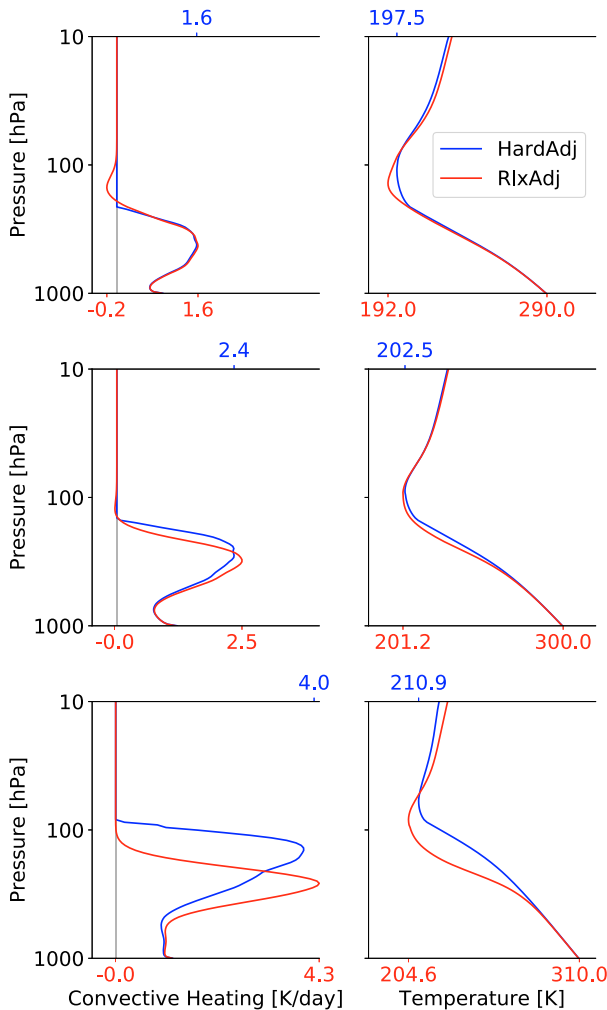


FIG. 2. Convective heating rate and temperature profiles for the hard (blue) and relaxed (red) convective adjustments with surface temperatures fixed at (top) 290, (middle) 300, and (bottom) 310 K. Surface and cold-point temperatures are indicated, as are minimum and maximum convective heating rates.

adjustment means that other factors have more influence on the TTL. More generally, we can investigate whether the way convection is treated affects the results of any of our experiments.

Our choice of $\tau(p)$ [Eq. (5)] produces an equilibrium surface temperature of 297.7, 0.2 K colder than the hard adjustment, and a cold-point temperature of 200.1, 1.2 K colder than that for the hard adjustment. Around the TTL, the relaxed convective adjustment provides a cooling (top row of Fig. 2), which results simply from following the moist adiabatic lapse rate. Thinking about this in terms of a rising air parcel, the parcel follows the moist adiabatic lapse rate and will overshoot its level of neutral buoyancy if it reaches this altitude with enough momentum. Convective cooling of the TTL is not present

in the hard adjustment, where the convective adjustment stops abruptly at the level of neutral buoyancy. In a warmer climate, the convective cooling is reduced in the relaxed adjustment with our definition of τ , as the level of neutral buoyancy occurs at a lower pressure where the convective time scale is larger.

Allowing for convective cooling above the level of neutral buoyancy may make the relaxed adjustment seem more realistic than the hard adjustment. However, as already noted, it is tuned to our standard model setup. Furthermore, in the upper troposphere, the relaxed adjustment produces temperatures that decrease more quickly with height than the moist adiabat, whereas observations show deviations from the moist adiabat in the opposite direction (e.g., Fig. 2 of Fueglistaler et al. 2009). In this sense, the relaxed adjustment is less realistic than the hard adjustment, which produces temperature profiles that exactly follow the moist adiabat.

b. Convective-top definition

In previous studies (Thuburn and Craig 2002; Birner and Charlesworth 2017), the convective top was defined, for the hard adjustment case, as the highest level to which a convective adjustment was applied. However, this definition suffers from the discrete nature of the model levels, and convective-top temperature values depend on the resolution. To resolve this issue, we perform an interpolation, defining the convective-top temperature as the temperature corresponding to a convective heating of 0.2 K day^{-1} . The value of 0.2 was chosen to be small, so that our convective top is close to the top level of our convective adjustment, where convective heating goes to zero. On the other hand, the chosen value needed to be far enough from zero for the interpolation to completely remove the effect of the zero convective heating level being at a discrete model level. Then, for consistency, the same definition can be used for the relaxed convective adjustment case, where there is no hard transition to radiative equilibrium.

3. Increasing CO_2

In this section, we study the effect of changing the CO_2 concentration on the TTL. Standard runs are performed with 348 ppmv CO_2 [the standard value for the proposed Radiative–Convective Equilibrium Model Intercomparison Project (RCEMIP); Wing et al. 2018] and in these sensitivity experiments we use values in the range [0.25, 4] times this amount.

Performing runs with a fixed surface temperature we see little change in the temperature, height or shape of the TTL (not shown), in agreement with Thuburn and Craig (2002) and Fu et al. (2018), who used a hard

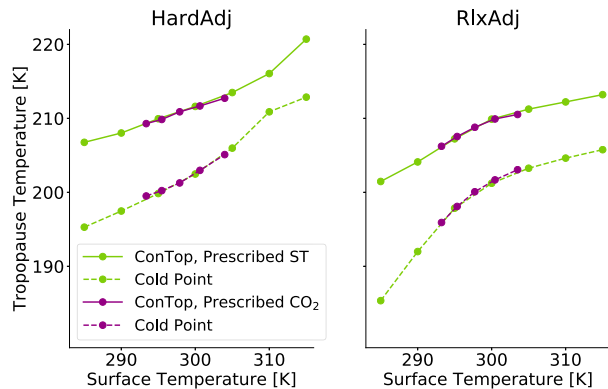


FIG. 3. Temperature of the convective top (solid) and the cold point (dashed) plotted against the surface temperature. Changes in TTL temperature and structure due to CO₂ changes (dark purple) are very similar to those found when simply fixing the surface temperature at higher values (pale green).

convective adjustment to a lapse rate of 6.5 K km^{-1} . This is the case for both our hard convective adjustment and our relaxed adjustment.

In contrast, if we allow the surface temperature to change, an increase in CO₂ concentration produces an increase in temperature and height of both the convective top (as shown by Kluft et al. 2019) and the cold point. We perform additional experiments with a fixed CO₂ concentration and a fixed surface temperature and use a different surface temperature for each run. We see a very similar response of TTL temperatures to increasing surface temperature as to increasing CO₂ concentration (Fig. 3). This suggests that at equilibrium TTL temperatures are intrinsically linked to surface and tropospheric temperatures. For other scenarios, such as when a Brewer–Dobson–like dynamical cooling term is applied, an increase in CO₂ has a different effect on TTL temperatures than an equivalent increase in surface temperature (section 6).

In the relaxed convective adjustment case, the upper troposphere and TTL is colder than in the hard adjustment case, as discussed in section 2. Additionally, the changes in cold-point temperature with surface temperature change are larger in the relaxed adjustment case for temperatures in the range [285, 300] K. A warming climate produces a rising TTL, and as the TTL rises, convective cooling becomes weaker, (cf. the negative convective heating values in the top-left and middle-left panels of Fig. 2), leading to a stronger warming of the TTL compared to the hard adjustment case. This effect is not so strong for the convective top, due to its definition at a fixed convective heating rate (section 2b). Conversely, for higher surface temperatures, [300, 315] K, the changes in convective top and cold-point temperature are smaller in the relaxed than

the hard adjustment case. In this temperature range, the longwave cooling is stronger and the troposphere is deeper, so with further increases in surface temperature the convective warming becomes less and less effective at balancing the radiative cooling in the upper troposphere. This causes the temperature profiles to deviate strongly from the moist adiabat (bottom two rows of Fig. 2), with radiation acting to cool the upper troposphere. This results in a cooler TTL than if convection were very efficient (adjusting strictly to the moist adiabatic lapse rate as in the hard adjustment case). We conclude that the assumptions relating to the convective adjustment strongly influence the structure of the TTL and its response to warming.

4. Ozone profile changes

In this set of experiments, we prescribe a variety of idealized ozone profiles, which have been shifted with respect to our standard profile from Wing et al. (2018) (Fig. 4). An upward-shifted profile could be expected under global warming as the troposphere expands, and this effect would be enhanced if the Brewer–Dobson circulation strengthens, bringing more ozone-poor air upward. We apply a range of perturbations to the ozone profile, some of which are much larger than what might be expected in a $4\times$ CO₂ scenario (see section 8), to improve our understanding. We also consider the opposite cases, in which the ozone profile is shifted downward, unrealistically allowing ozone rich air into the upper troposphere. The temperature and humidity profiles which result from shifting the ozone profile are also shown in Fig. 4. These experiments are similar to the runs of Birner and Charlesworth (2017), Thuburn and Craig (2002), and McElroy et al. (1992) and indeed our results are similar to theirs for the TTL. Both the convective top and the cold point increase in height and decrease in temperature when the ozone profile is shifted upward, due to a reduction of radiative heating in this region (approximately in the range [200, 10] hPa). The TTL changes are almost the same for the runs with fixed surface temperature (not shown) and those with variable surface temperature. Qualitatively similar results were found for the hard and relaxed convective adjustment cases.

We also investigate the effect that shifting the ozone profile has on the surface temperature (Fig. 5) and find that a downward-shifted ozone profile is associated with an increase in surface temperature and an upward-shifted profile with a somewhat smaller decrease. Our surface temperature changes are larger than those of McElroy et al. (1992), which is somewhat surprising

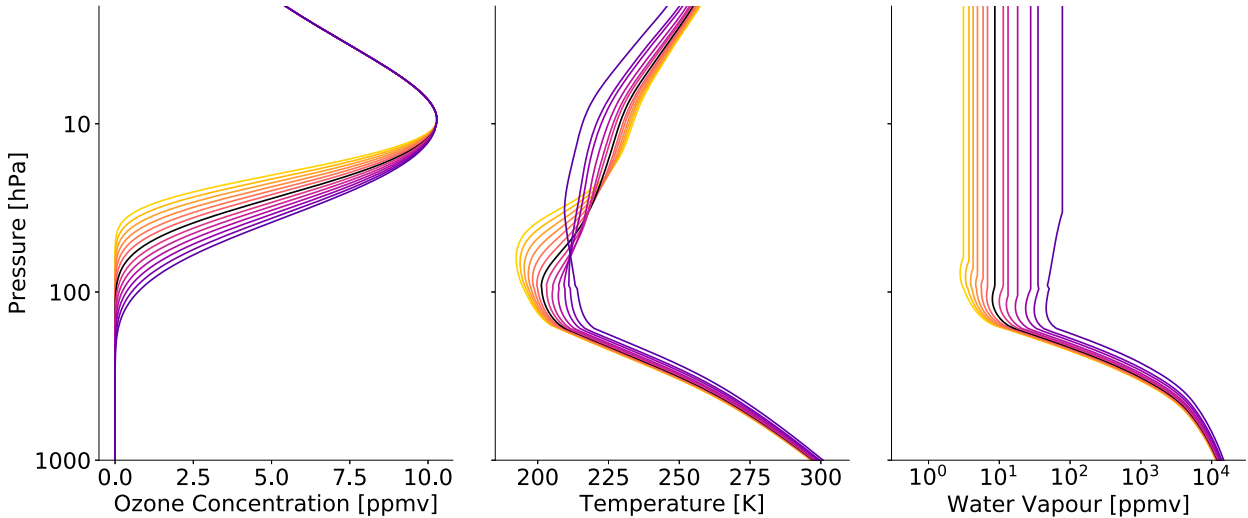


FIG. 4. Artificial changes to (left) the ozone concentration profile and the corresponding changes to (center) the temperature and (right) the water vapor profiles for the hard convective adjustment case. The black lines indicate the standard profiles, and the yellow lines correspond to an upward shift in the ozone profile, as might be expected under global warming.

given the similarities in the model setup and the additional lapse-rate feedback in our model which acts to weaken the surface temperature response.

We expected that the solar insolation may play a role in the strength of the response to changes in the ozone profile, so we test this in runs with an applied constant heat sink at the surface such that the reference climate remains approximately constant. With a stronger insolation, shortwave heating increases, especially around the stratopause. However, we find little difference in the tropopause and surface–tropospheric temperature response to ozone, suggesting that ozone-induced changes occur through longwave heating changes.

In our model, we find that the surface temperature changes due to the radiative effects of ozone alone are small (fVMR in Fig. 5), but that these are amplified by the water vapor response by a factor between 4.8 and 7.9 for the upward-shifted profiles and up to 10.0 for the downward-shifted profiles (cf. fRH and fVMR in Fig. 5). Cooling of TTL temperatures due to an upward shift in the ozone profile (discussed above) leads to a reduction in water vapor content of the air in this region (Fig. 4). This acts to both reduce the greenhouse effect and to destabilize the TTL and upper troposphere, leading to increased convection, both of which produce surface cooling. Tropospheric temperatures also cool and this causes a reduction in tropospheric water vapor, which further reduces the surface temperature.

5. Upwelling

Birner and Charlesworth (2017) found that their RCE model overestimated TTL temperatures by up to ~ 15 K

when no dynamical stratospheric cooling was applied (see, e.g., their Fig. 3). With a cooling term corresponding to an upwelling velocity of 0.5 mm s^{-1} everywhere above the convective top, mimicking the Brewer–Dobson circulation, they found temperatures much closer to those observed (their Fig. 11). We repeat their experiments with two different upwelling velocities: 0.5 mm s^{-1} , which is close to estimates of upwelling velocities from reanalysis (Abalos et al. 2015) at ~ 100 hPa (although it varies above this), and an intermediate value of 0.25 mm s^{-1} . Additionally, we study how the upwelling affects surface temperature. We use the same equation as Birner and Charlesworth (2017) for the dynamical cooling rate:

$$Q = -w \left(\frac{\partial T}{\partial z} + \frac{g}{C_p} \right), \quad (6)$$

where w is a prescribed upwelling velocity, T is temperature, z is altitude, g is gravity, and C_p is isobaric heat capacity, with g and C_p approximated as constants.

In these experiments energy is constantly being removed due to this stratospheric cooling term, and this is balanced by a nonzero net flux at the top of the atmosphere. In the real atmosphere, this would be compensated for in the extratropics. In addition, there is no transport: gas concentrations are treated as before (described in section 2).

As shown in Fig. 6 and found by Birner and Charlesworth (2017), including a dynamical cooling term reduces TTL temperatures, and makes the cold point sharper. Although the cooling is applied everywhere above the convective top, it mainly affects the

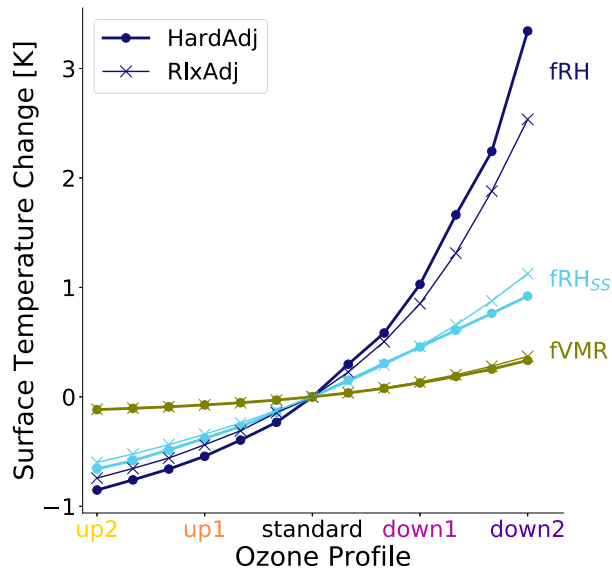


FIG. 5. Surface temperature changes corresponding to artificially shifted ozone profiles, with negative surface temperature changes on the left corresponding to an upward shift (yellow in Fig. 4) and positive temperature changes on the right to a downward shift (purple in Fig. 4). Dots and crosses correspond to experiments with the hard convective adjustment (HardAdj) and the relaxed adjustment (RlxAdj), respectively. The different colors of the lines and markers are for the different treatment of water vapor. The standard treatment, with fixed relative humidity in the troposphere and stratospheric humidity set by the cold point, is indicated by “fRH.” Runs with fixed relative humidity in the troposphere but a constant specified stratospheric water vapor mixing ratio are labeled as “fRHss.” Runs with a fixed water vapor volume mixing ratio at each pressure level throughout the column are labeled as “fVMR.”

TTL region and lower stratosphere, as above radiative heating is very efficient at maintaining the atmosphere near radiative equilibrium.

Larger upwelling velocities also act to cool the modeled tropical surface and troposphere, and as for ozone profile effects on the surface (section 4), these changes occur mainly through changes in water vapor content (Table 1). The applied upwelling acts to lift the TTL, as well as to cool it. While a cooling of the TTL would be associated with a cooler troposphere and surface (due to their connection via the specified lapse rate), a higher TTL leads to a warmer troposphere and surface (following the same reasoning). For the fVMR cases studied here, the two factors almost cancel and the surface temperature changes little. When water vapor is allowed to vary, a cooling of the TTL (and therefore also troposphere and surface) would be associated with a drying of the whole atmospheric column. On the other hand, a lifting of the cold point to a lower pressure leads to an increase in stratospheric water vapor, as the conversion from relative humidity (fixed at 0.4) depends on

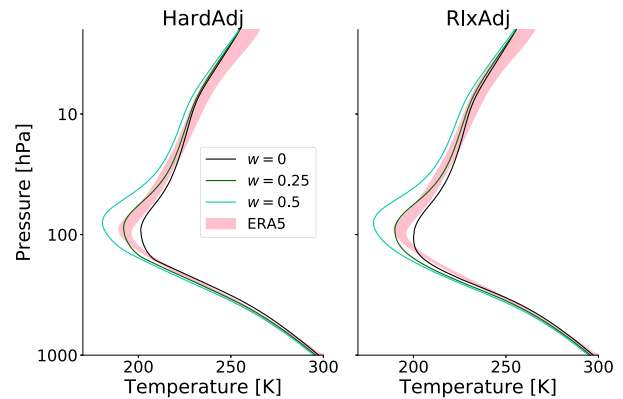


FIG. 6. Temperature profiles for runs with different stratospheric upwelling velocities. The standard setup with no upwelling is shown in black and runs with upwelling velocities of 0.25 and 0.5 mm s^{-1} are shown in dark and light green, respectively. Pink shading shows ERA5 data within one standard deviation of the mean tropical temperature profile.

pressure. This leads to a slight warming of the cold point in the fRH case compared to the fVMR case. For the convective-top and surface temperatures, the decrease in tropospheric humidity has a larger effect than the increase in stratospheric humidity, leading to a much larger cooling for fRH than fVMR.

To summarize, there are two main competing factors affecting the surface temperature in the fRH case: a warming due to an increase in altitude of the TTL and the requirement to follow the moist adiabatic lapse rate in the troposphere, and a cooling due to the decrease in temperature of TTL and the associated reduction in water vapor content.

6. Combined effects

It is also of interest to study combined cases, for example an increase in CO_2 together with an upward-shifted ozone profile. One might naively assume that the total effect would be the sum of the individual effects, and if this were the case we could say that the factors act

TABLE 1. Temperature changes (K) associated with different upwelling velocities w (mm s^{-1}), compared to the case with no upwelling. Values for the hard adjustment are given in boldface font, and those for the relaxed adjustment in normal font. Results are shown for both runs with fixed tropospheric relative humidity (fRH) and runs with fixed water vapor mixing ratio (fVMR).

w	Run	Cold point		ConTop		Surface	
0.25	fRH	-9.3	-10.1	-6.0	-5.4	-1.5	-1.5
	fVMR	-10.1	-10.3	-3.8	-4.0	-0.3	-0.3
0.5	fRH	-20.7	-21.7	-11.2	-9.6	-2.5	-2.5
	fVMR	-19.2	-20.2	-6.6	-6.9	-0.4	-0.5

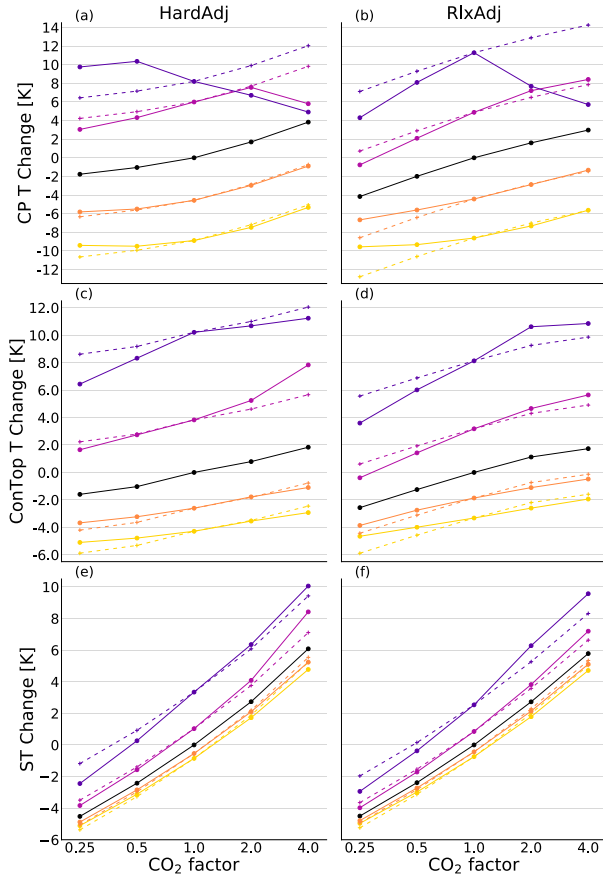


FIG. 7. (a),(b) Cold-point, (c),(d) convective-top, and (e),(f) surface temperature changes with increasing CO_2 and different ozone profiles. The ozone profile used is indicated by the color, with black representing the standard profile, pink and purple representing downward-shifted profiles (down1 and down2, respectively; see Fig. 5), and orange and yellow representing upward-shifted profiles (up1 and up2, respectively). (left) Results for the setup with the hard convective adjustment, and (right) those with the relaxed convective adjustment. Dashed lines and crosses show the predicted behavior assuming additivity and solid lines and dots show the actual behavior.

independently of each other. In this section, we investigate whether and under which conditions such a summation provides a good prediction for the combined effect.

Figure 7 shows the combined effect of a change in CO_2 concentration and a shifted ozone profile. The predicted trends (dashed), calculated by summation of the temperature changes found in sections 3 and 4, are close to the temperature changes for runs where both factors are changed simultaneously (colored solid lines) in some parts of the parameter space. Similar results are found for the interaction between CO_2 and ozone also for cases with applied stratospheric upwelling velocities of 0.25 and 0.5 mm s^{-1} (not shown). However, there are some extreme cases (seen in all three upwelling scenarios),

TABLE 2. Temperature changes (K) associated with a doubling of CO_2 (696 vs 348 ppmv) for different upwelling velocities w (mm s^{-1}). Values for the hard adjustment are given in boldface font, and those for the relaxed adjustment in normal font.

w	Cold point	ConTop	Surface
0	1.7	1.6	0.8
0.25	3.6	3.4	1.4
0.5	4.9	4.0	1.8

where the effects of ozone and CO_2 cannot be considered independent. One such example is the cold-point temperature for a strongly downward-shifted ozone profile and an increase in CO_2 in both the hard and relaxed adjustment cases (Fig. 7a). The cooler stratosphere associated with an increase in CO_2 leads to a less distinct TTL region, and when the ozone profile is simultaneously shifted downward, the resultant warming beneath the cold point causes it to jump to a significantly higher altitude.

There are also notable differences in convective-top temperature trends for the relaxed adjustment case, namely, that the sensitivity to ozone depends on CO_2 concentration (the solid lines in Fig. 7d diverge with increasing CO_2). For a larger CO_2 concentration, the convective top is at a lower pressure (higher altitude), where the ozone changes are more significant than at higher pressures where ozone concentrations are always low.

The assumption of additivity is quite good for the surface temperature (bottom panels of Fig. 7), where the predicted behavior (dashed) closely matches the actual behavior (solid). In other words, the effect of CO_2 on surface temperature is nearly independent of the prescribed ozone profile.

Likewise, we find that surface temperature changes due to changes in CO_2 concentration are almost independent of the applied stratospheric dynamical cooling term (Table 2). Conversely, the upwelling term significantly alters cold-point temperature trends with changing CO_2 concentration or shifting the ozone profile (Tables 2 and 3). The warming of the cold point corresponding to a doubling of CO_2 increases for larger upwelling velocities, and there are two main processes contributing to this. One can be explained through an alteration of the relationship between surface temperature and TTL temperature when an upwelling is applied. To balance an increase in upwelling longwave radiation from below, a colder tropopause layer must undergo a larger increase in temperature than a tropopause layer which is initially warmer. The other is related to the calculation of the cooling term associated with the upwelling, which depends on the temperature gradient. By cooling the stratosphere, CO_2 reduces the

TABLE 3. Temperature changes (K) associated with an upward shift of the ozone profile (up1 from Fig. 5) for different upwelling velocities w (mm s^{-1}). Values for the hard adjustment are given in boldface font, and those for the relaxed adjustment in normal font.

w	Cold point		ConTop		Surface	
0	-4.6	-4.4	-2.6	-1.9	-0.5	-0.4
0.25	-7.0	-6.4	-2.4	-1.8	-0.3	-0.3
0.5	-8.4	-8.6	-2.3	-1.6	-0.1	-0.1

temperature gradient particularly in the lower stratosphere and this reduces the adiabatic cooling term there [Eq. (6)]. Reduction in this cooling term produces an apparent warming just above the cold point, which then leads to an additional warming of the cold point through radiative transfer. For these cases, there is an influence of CO_2 induced stratospheric cooling on the cold-point temperature, unlike in the case with no upwelling where the cold-point temperature is found to depend almost exclusively on surface temperature (Fig. 3).

The cold-point sensitivity to an upward shift in the ozone profile increases under stronger upwelling velocities (Table 3). The upwelling lofts the cold point, bringing it closer to the large ozone gradient, where larger changes in ozone concentration occur when a vertical shift to the profile is applied. A second contribution comes from the increase in longwave heating by ozone at colder temperatures, so any changes in ozone concentration have a larger impact. However, the colder TTL produced when an upwelling is applied contains less water vapor, so changes in the ozone profile are associated with relatively small changes in water vapor concentration. As most of the ozone effect on the surface is through water vapor changes (Fig. 5), the surface sensitivity to ozone decreases for cases with strong upwelling velocities.

In summary, ozone and CO_2 act almost independently of each other for some parts of the parameter space tested, but in other parts, the assumption of additivity is a bad one. Likewise, using a different upwelling velocity in the model affects the response of the column atmosphere to changes in our prescribed ozone and CO_2 concentrations.

7. Temporal evolution of the cold point

In this section, we investigate how the system evolves over time and how initial responses relate to equilibrium states. When considering a local temperature response to an instantaneous forcing (e.g., a CO_2 perturbation), it is important to keep in mind that the entire column can adjust and therefore that the local temperature response at a later time cannot necessarily be inferred from the

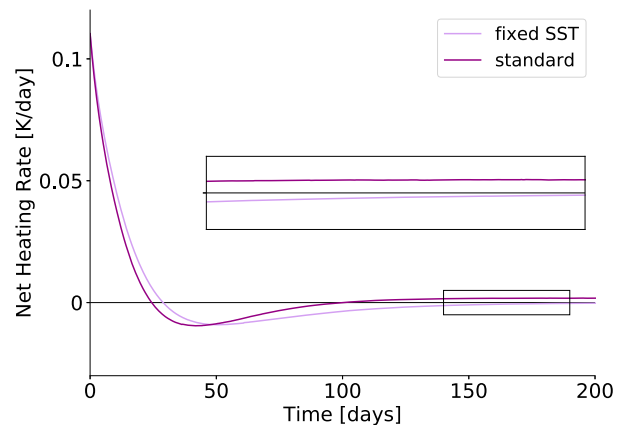


FIG. 8. Net radiative heating rates at the cold point after a $4\times\text{CO}_2$ perturbation and their evolution with time for two different model setups.

initial heating rate at that location. If the temperature initially responds by warming, one might assume that it continues warming, albeit at a slower rate, until equilibrium is reached. Likewise, if it cools, one might assume that it continues cooling until equilibrium is reached. By making such an assumption, the column response is considered of little or no importance for the local response. This proves reasonable for the surface in our 1D model, which, after a positive radiative forcing is applied, warms slowly and with a rate of warming that decreases toward zero as the forcing decreases toward zero. Here we investigate whether such an assumption is also appropriate for the tropopause, by studying the specific case of cold-point evolution under an instantaneous CO_2 perturbation.

Two sets of experiments are used, one with the standard setup, hard convective adjustment and CO_2 prescribed at 0.25, 0.5, 2, or 4 times our standard concentration (348 ppmv), and another set where we fix the surface temperature and the absolute humidity. In the second set of experiments, the only variable that can change is temperature and this is fixed in the troposphere due to the fixed surface temperature and our hard convective adjustment. The runs are initialized using the equilibrium state of the standard $1\times\text{CO}_2$ run. Figure 8 shows the evolution of the net radiative heating rate at the cold point for the $4\times\text{CO}_2$ runs. In all these experiments, the net radiative heating rate translates directly into a subsequent change in temperature of the cold point, as there is no upwelling and also no convection affecting the temperature at this altitude.

With increased CO_2 , we find a net positive heating rate at the cold point for the first ~ 30 model days. This agrees with the results of Lin et al. (2017), who calculated radiative heating rates for a single tropical-mean temperature

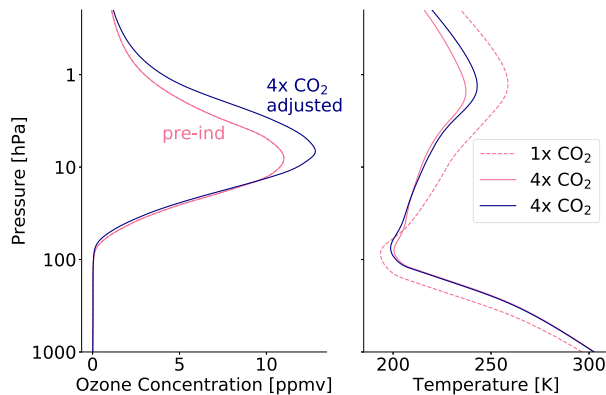


FIG. 9. (right) Temperature profiles from our 1D RCE when using (left) the ozone profiles from Marsh et al. (2016). The dashed-pink temperature profile in the left panel is from that found for the run with $1\times\text{CO}_2$ and the preindustrial ozone profile (pink). The solid-pink and blue temperature profiles are from runs with $4\times\text{CO}_2$ and the ozone profiles of corresponding colors.

profile under a variety of CO_2 concentrations. However, as the temperature profile evolves and the stratosphere cools, the heating rate anomaly at the cold point decreases, becoming negative, before increasing again toward zero as the simulation reaches equilibrium. As the stratosphere cools, the net radiative forcing on the tropopause decreases and the initial positive temperature perturbation reduces. With decreased CO_2 the opposite evolution is found (not shown), namely an initial cooling and a subsequent warming as the stratosphere warms.

Both sets of experiments show a similar evolution during the first approximately 100 model days, suggesting that changes in TTL and stratospheric temperatures are responsible for the early evolution, while changes in humidity or surface and tropospheric temperatures have little influence. The initial warming and subsequent cooling approximately cancel and the cold-point temperature after approximately 100 days is almost the same as the initial cold-point temperature. This contradicts the assumption that an initial warming leads to a warmer temperature at any later time in the evolution compared to the initial state.

Differences between the two sets of experiments only occur during the later evolution (zoom box of Fig. 8), where in the fixed surface temperature case, the net heating rate at the cold point quickly reaches zero, but when the surface temperature is allowed to change, the cold point warms slowly as the surface warms, until both the surface and the cold point eventually reach equilibrium (not shown). The relationship between surface temperature and tropopause temperature found in section 3 only holds after the initial adjustment period, while during the initial adjustment time the influence of the stratosphere must be taken into account.

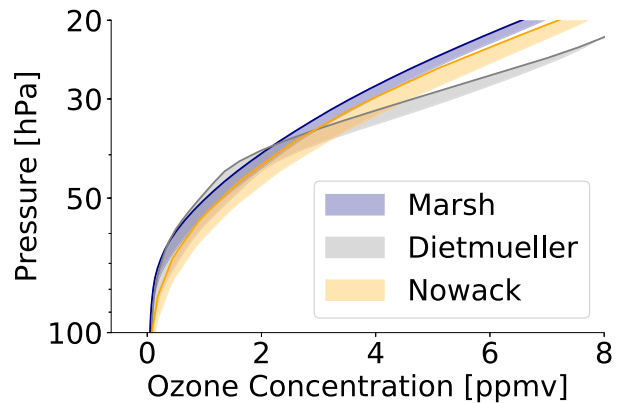


FIG. 10. Tropical-mean lower-stratospheric ozone profiles from the coupled chemistry–climate models of Marsh et al. (2016), Dietmüller et al. (2014), and Nowack et al. (2015). The solid lines indicate the profiles in the $4\times\text{CO}_2$ scenarios, and the shading shows the change from the $1\times\text{CO}_2$ runs.

8. The importance of ozone and the model setup

To put our model into context with other studies and to see the influence of the model setup in a more tangible example, we use the tropical-mean ozone profiles from the interactive chemistry preindustrial and $4\times\text{CO}_2$ runs of Marsh et al. (2016), Dietmüller et al. (2014), and Nowack et al. (2015). The two ozone profiles of Marsh et al. (2016) are shown in the left panel of Fig. 9, labeled as “pre-ind” and “ $4\times\text{CO}_2$ ” adjusted, respectively. A large increase in ozone concentration is apparent in the upper stratosphere, due to CO_2 induced cooling, but this is not expected to have much impact on tropospheric and TTL temperatures, as the absolute ozone concentrations are small here. In the lower stratosphere, a small upward shift in the ozone profile can be seen (Fig. 10), similar to the idealized ozone profiles of section 4.

The right panel of Fig. 9 shows the equilibrium temperature profiles produced in our model using the hard convective adjustment and an upwelling velocity of 0.25 mm s^{-1} . In this case, the cold-point temperature increase when increasing the CO_2 by a factor of 4 and changing the ozone profile from the preindustrial to the adjusted profile is 5.2 K compared with 7.0 K when keeping the preindustrial ozone profile. We find corresponding surface temperature changes of about 6.0 and 6.3 K, and it follows that the adjusted ozone profile produces a decrease in surface temperature of 0.3 K compared to the preindustrial profile. Performing the same analysis with ozone profiles from Dietmüller et al. (2014) and Nowack et al. (2015) gives decreases in surface temperature of 0.4 and 0.6 K, respectively. The differing results suggest that some, but not all, of the discrepancy between the global modeling studies (Marsh et al. 2016; Dietmüller et al. 2014; Nowack et al. 2015) can be

TABLE 4. Change in surface temperature (K) under a $4\times\text{CO}_2$ scenario (left value) and the change in this (K) when using an ozone profile from a $4\times\text{CO}_2$ simulation compared to the climatology ozone profile (right value). Ozone profiles are from the coupled chemistry–climate models of Marsh et al. (2016), Dietmüller et al. (2014), and Nowack et al. (2015). Results are shown for three different configurations of our 1D model: the first row may be considered our best estimate, the second row neglects upwelling, and the third both neglects upwelling and uses the relative humidity profile from Manabe and Wetherald (1967) and Kluft et al. (2019).

	Marsh		Dietmüller		Nowack	
$w = 0.25$	6.3	−0.3	6.5	−0.4	6.6	−0.6
$w = 0$	6.3	−0.4	6.5	−0.6	7.1	−1.1
Manabe RH	4.3	−0.2	4.3	−0.2	4.3	−0.3

explained by differences in their ozone profiles (Fig. 10). However, from this study it is not possible to tell whether these differences arise due to the ozone schemes, the model top [relatively low in Dietmüller et al. (2014)] or the background state, including temperature profile and circulation, of the global climate models.

The results stated above may be considered the best estimates we can make with our simple model, with upper-tropospheric relative humidity and TTL temperatures of the $1\times\text{CO}_2$ state in approximate agreement with ERA5 data (Fig. 6). However, it is clear that many processes are missing from our model (e.g., clouds) and that several of our model assumptions are overly simplistic. Changing some of these assumptions to ones that have been used in previous 1D RCE studies drastically affects the influence of ozone (Table 4). Changing the humidity profile also has a large impact on the climate sensitivity itself and a more detailed study of this can be found in Kluft et al. (2019). Neglecting upwelling produces a TTL that is warmer than observed and using the tropospheric relative humidity profile from Manabe and Wetherald (1967) produces an upper troposphere that is drier than observed. It is important that both temperature and humidity (particularly in the upper troposphere and lower stratosphere) are well represented in order to obtain reasonable results regarding the influence of changes in ozone.

9. Discussion and conclusions

In our 1D model, we find that several factors influence the structure of the TTL, with an increase in CO_2 acting to warm it and an upward shift in the ozone profile acting to cool it. An applied stratospheric dynamical cooling also acts to reduce TTL temperatures, as does a convective adjustment that takes into account cooling aloft. In addition, we investigate the interplay of the different factors, and find that the choice of upwelling velocity and

convective adjustment treatment both affect how changes in the gas concentrations affect TTL temperatures. Further, the ability to accurately predict the combined effect of CO_2 and ozone from their individual effects depends on the convective adjustment method. Even in our relatively simple model setup, we show that a number of factors play a significant role for the TTL and that they interact in a complicated way, which may help to explain disagreements in global model predictions of TTL evolution. Moreover, the temporal response of the TTL depends on processes occurring on different time scales, adding additional complications to predicting TTL evolution under realistic forcing conditions, when the stratosphere is not equilibrated.

Studying surface temperature response to CO_2 in our model, we find only a small dependence on the model setup [aside from the humidity profile as shown in Table 4 and Kluft et al. (2019)], with the type of convective adjustment and strength of upwelling velocity having relatively little impact. This suggests that climate sensitivity is quite robust to differences in TTL structure and evolution. On the other hand, the type of convective adjustment and strength of upwelling play a role when studying surface temperature response to a shift in the ozone profile. Water vapor feedbacks have a strong effect here, and when no upwelling is applied, they amplify the surface temperature response to a shift in the ozone profile by a factor between 4.8 and 10.0, depending on the method of convective adjustment and the size of the ozone shift. When considering ozone profile changes that might be expected from a $4\times\text{CO}_2$ scenario (from Marsh et al. 2016; Dietmüller et al. 2014; Nowack et al. 2015), we find a surface temperature decrease between ~ 0.3 and 0.6 K, compared to an increase in temperature from the quadrupling of CO_2 of >6 K. In this context, we show a relatively small influence of a perturbation applied at and above the TTL on the surface temperature.

A main advantage of using 1D RCE models is to disentangle the different processes, and this can be done simply by running the model under different configurations. In comparison, to separate the effect of different factors in complex modeling studies, researchers may interpret their results or use analysis methods based on the assumptions that the various factors act independently from one another, and that an initial warming is followed by continuous warming until equilibrium is reached. As we show in sections 6 and 7, these are not always reasonable assumptions, so care must be taken, particularly when studying the tropopause layer.

We show that idealized models can be a useful tool to help understand processes and to test assumptions used in models or analysis methods. On the other hand, the

highly idealized nature of 1D RCE models means that many processes are simplified (such as convection, or treatment of stratospheric water vapor) or not included at all. In global models and the real world, circulation changes would likely occur as a response to changes in radiative forcing, and these could have a feedback effect on the climate, regionally or even globally. Further, our model does not include clouds, which may be affected by ozone or residual circulation changes. If we use our convective top as a proxy for the tropical high cloud detrainment level, we can see that an upward-shifted ozone profile or an increased upwelling decreases the cloud temperature, which would increase the positive cloud longwave feedback [following the reasoning of Zelinka and Hartmann (2010)]. A more detailed investigation, preferably using a convection-resolving model, would be needed to quantify the strength of this effect.

Acknowledgments. Thanks to Dan Marsh for providing the ozone profiles used for Fig. 9 and shown in Fig. 10. Thanks to Michael Ponater for interesting discussions and to Katharina Meraner and four reviewers for their constructive comments. Thanks also to the developers of CliMT (Monteiro et al. 2018), a python package that enables the easy use of the RRTMG radiation scheme. Stefan Buehler is supported by the Cluster of Excellence CliSAP (EXC177), Universität Hamburg, funded by the German Science Foundation (DFG). Peer Nowack is supported through an Imperial College Research Fellowship.

REFERENCES

- Abalos, M., B. Legras, F. Ploeger, and W. J. Randel, 2015: Evaluating the advective Brewer–Dobson circulation in three reanalyses for the period 1979–2012. *J. Geophys. Res. Atmos.*, **120**, 7534–7554, <https://doi.org/10.1002/2015JD023182>.
- Betts, A., and M. Miller, 1986: A new convective adjustment scheme. Part II: Single column tests using gate wave, BOMEX, ATEX and arctic air-mass data sets. *Quart. J. Roy. Meteor. Soc.*, **112**, 693–709, <https://doi.org/10.1002/QJ.49711247308>.
- Birner, T., and E. J. Charlesworth, 2017: On the relative importance of radiative and dynamical heating for tropical tropopause temperatures. *J. Geophys. Res. Atmos.*, **122**, 6782–6797, <https://doi.org/10.1002/2016JD026445>.
- Butchart, N., and Coauthors, 2006: Simulations of anthropogenic change in the strength of the Brewer–Dobson circulation. *Climate Dyn.*, **27**, 727–741, <https://doi.org/10.1007/s00382-006-0162-4>.
- Dietmüller, S., M. Ponater, and R. Sausen, 2014: Interactive ozone induces a negative feedback in CO₂-driven climate change simulations. *J. Geophys. Res. Atmos.*, **119**, 1796–1805, <https://doi.org/10.1002/2013JD020575>.
- Dobson, G. M. B., A. Brewer, and B. Cwilong, 1946: Bakerian lecture: Meteorology of the lower stratosphere. *Proc. Roy. Soc. London*, **185A**, 144–175, <https://doi.org/10.1098/rspa.1946.0010>.
- Fu, Q., M. Smith, and Q. Yang, 2018: The impact of cloud radiative effects on the tropical tropopause layer temperatures. *Atmosphere*, **9**, 377, <https://doi.org/10.3390/atmos9100377>.
- Fueglistaler, S., A. Dessler, T. Dunkerton, I. Folkins, Q. Fu, and P. W. Mote, 2009: Tropical tropopause layer. *Rev. Geophys.*, **47**, RG1004, <https://doi.org/10.1029/2008RG000267>.
- Garcia, R. R., and W. J. Randel, 2008: Acceleration of the Brewer–Dobson circulation due to increases in greenhouse gases. *J. Atmos. Sci.*, **65**, 2731–2739, <https://doi.org/10.1175/2008JAS2712.1>.
- Gottelman, A., and Coauthors, 2010: Multimodel assessment of the upper troposphere and lower stratosphere: Tropics and global trends. *J. Geophys. Res.*, **115**, D00M08, <https://doi.org/10.1029/2009JD013638>.
- Gowan, E., 1947: Ozonosphere temperatures under radiation equilibrium. *Proc. Roy. Soc. London*, **190A**, 219–226, <https://doi.org/10.1098/rspa.1947.0071>.
- Holloway, C. E., and J. D. Neelin, 2007: The convective cold top and quasi equilibrium. *J. Atmos. Sci.*, **64**, 1467–1487, <https://doi.org/10.1175/JAS3907.1>.
- Hummel, J., and W. Kuhn, 1981: Comparison of radiative-convective models with constant and pressure-dependent lapse rates. *Tellus*, **33**, 254–261, <https://doi.org/10.3402/tellusa.v33i3.10713>.
- Johnson, R. H., and D. C. Kriete, 1982: Thermodynamic and circulation characteristics of winter monsoon tropical mesoscale convection. *Mon. Wea. Rev.*, **110**, 1898–1911, [https://doi.org/10.1175/1520-0493\(1982\)110<1898:TACCOW>2.0.CO;2](https://doi.org/10.1175/1520-0493(1982)110<1898:TACCOW>2.0.CO;2).
- Kim, J., K. M. Grise, and S.-W. Son, 2013: Thermal characteristics of the cold-point tropopause region in CMIP5 models. *J. Geophys. Res. Atmos.*, **118**, 8827–8841, <https://doi.org/10.1002/JGRD.50649>.
- Kluft, L., S. Dacie, S. A. Buehler, H. Schmidt, and B. Stevens, 2019: Reexamining the first climate models: Climate sensitivity of a modern radiative–convective equilibrium model. *J. Climate*, <https://doi.org/10.1175/JCLI-D-18-0774.1>, in press.
- Kuang, Z., and C. S. Bretherton, 2004: Convective influence on the heat balance of the tropical tropopause layer: A cloud-resolving model study. *J. Atmos. Sci.*, **61**, 2919–2927, <https://doi.org/10.1175/JAS-3306.1>.
- Lin, P., D. Paynter, Y. Ming, and V. Ramaswamy, 2017: Changes of the tropical tropopause layer under global warming. *J. Climate*, **30**, 1245–1258, <https://doi.org/10.1175/JCLI-D-16-0457.1>.
- Manabe, S., and F. Möller, 1961: On the radiative equilibrium and heat balance of the atmosphere. *Mon. Wea. Rev.*, [https://doi.org/10.1175/1520-0493\(1961\)089<0503:OTREAH>2.0.CO;2](https://doi.org/10.1175/1520-0493(1961)089<0503:OTREAH>2.0.CO;2).
- , and R. T. Wetherald, 1967: Thermal equilibrium of the atmosphere with a given distribution of relative humidity. *J. Atmos. Sci.*, **24**, 241–259, [https://doi.org/10.1175/1520-0469\(1967\)024<0241:TEOTAW>2.0.CO;2](https://doi.org/10.1175/1520-0469(1967)024<0241:TEOTAW>2.0.CO;2).
- Marsh, D. R., J.-F. Lamarque, A. J. Conley, and L. M. Polvani, 2016: Stratospheric ozone chemistry feedbacks are not critical for the determination of climate sensitivity in CESM1(WACCM). *Geophys. Res. Lett.*, **43**, 3928–3934, <https://doi.org/10.1002/2016GL068344>.
- McElroy, M. B., R. J. Salawitch, and K. Minschwaner, 1992: The changing stratosphere. *Planet. Space Sci.*, **40**, 373–401, [https://doi.org/10.1016/0032-0633\(92\)90070-5](https://doi.org/10.1016/0032-0633(92)90070-5).
- Mlawer, E. J., S. J. Taubman, P. D. Brown, M. J. Iacono, and S. A. Clough, 1997: Radiative transfer for inhomogeneous atmospheres: RRTM, a validated correlated-k model for the longwave. *J. Geophys. Res.*, **102**, 16 663–16 682, <https://doi.org/10.1029/97JD00237>.
- Monteiro, J. M., J. McGibbon, and R. Caballero, 2018: sympl (v. 0.4. 0) and climt (v. 0.15. 3) – Towards a flexible framework for building model hierarchies in python. *Geosci. Model Dev.*, **11**, 3781–3794, <https://doi.org/10.5194/gmd-11-3781-2018>.

- Nowack, P. J., A. N. Luke, A. C. Maycock, P. Braesicke, J. M. Gregory, M. M. Joshi, A. Osprey, and J. A. Pyle, 2015: A large ozone–circulation feedback and its implications for global warming assessments. *Nat. Climate Change*, **5**, 41–45, <https://doi.org/10.1038/nclimate2451>.
- Oberländer-Hayn, S., and Coauthors, 2016: Is the Brewer–Dobson circulation increasing or moving upward? *Geophys. Res. Lett.*, **43**, 1772–1779, <https://doi.org/10.1002/2015GL067545>.
- Paulik, L. C., and T. Birner, 2012: Quantifying the deep convective temperature signal within the tropical tropopause layer (TTL). *Atmos. Chem. Phys.*, **12**, 12 183–12 195, <https://doi.org/10.5194/acp-12-12183-2012>.
- Romps, D. M., 2014: An analytical model for tropical relative humidity. *J. Climate*, **27**, 7432–7449, <https://doi.org/10.1175/JCLI-D-14-00255.1>.
- Sherwood, S. C., and A. E. Dessler, 2000: On the control of stratospheric humidity. *Geophys. Res. Lett.*, **27**, 2513–2516, <https://doi.org/10.1029/2000GL011438>.
- Son, S.-W., N. F. Tandon, and L. M. Polvani, 2011: The fine-scale structure of the global tropopause derived from COSMIC GPS radio occultation measurements. *J. Geophys. Res.*, **116**, D20113, <https://doi.org/10.1029/2011JD016030>.
- Thuburn, J., and G. Craig, 2002: On the temperature structure of the tropical stratosphere. *J. Geophys. Res.*, **107**, 4017, <https://doi.org/10.1029/2001JD000448>.
- Wang, J. S., D. J. Seidel, and M. Free, 2012: How well do we know recent climate trends at the tropical tropopause? *J. Geophys. Res.*, **117**, D09118, <https://doi.org/10.1029/2012JD017444>.
- Wing, A. A., K. A. Reed, M. Satoh, B. Stevens, S. Bony, and T. Ohno, 2018: Radiative-convective equilibrium model intercomparison project. *Geosci. Model Dev.*, **11**, 793–813, <https://doi.org/10.5194/gmd-11-793-2018>.
- Zelinka, M. D., and D. L. Hartmann, 2010: Why is longwave cloud feedback positive? *J. Geophys. Res.*, **115**, D16117, <https://doi.org/10.1029/2010JD013817>.